Atomic Force Microscopy Measurements of Adsorbed Polyelectrolyte Layers. 2. Effect of Composition and Substrate on Structure, Forces, and Friction

ARTICLE *in* LANGMUIR · APRIL 2003

Impact Factor: 4.46 · DOI: 10.1021/la026571h

3 AUTHORS, INCLUDING:

Adam Armitage Feiler
KTH Royal Institute of Technology
25 PUBLICATIONS **903** CITATIONS
SEE PROFILE

Mark W Rutland
KTH Royal Institute of Technology
148 PUBLICATIONS **3,564** CITATIONS
SEE PROFILE

Atomic Force Microscopy Measurements of Adsorbed Polyelectrolyte Layers. 2. Effect of Composition and Substrate on Structure, Forces, and Friction

Mark A. Plunkett, Adam Feiler, and Mark W. Rutland*

Department of Chemistry, Surface Chemistry, Royal Institute of Technology, SE-100 44 Stockholm, Sweden, and The Institute for Surface Chemistry, P.O. Box 5607, SE-11486 Stockholm, Sweden

Received September 17, 2002. In Final Form: March 5, 2003

An investigation on the effect of the conformation of preadsorbed polyelectrolyte layers of acrylamide−1% [3-(2-methylpropionamide)propyl]trimethylammonium chloride on the normal and lateral interactions between surfaces has been conducted. It was shown that when bridging mechanisms increased the adhesion, huge increases in the friction were also seen. When the polymer adsorbed in an extended layer, it resulted in a steric repulsion in the direction normal to the interface. However, the resulting friction measurements were shown to be far more complicated. For example, in cases where the integrity of the polymer layer was maintained under compression, the layer was able to act as a lubricant; however when the layer integrity was affected by the load and shear rate, then friction increased due to energy losses resulting from disrupting the polymer conformation. The conformation was controlled by varying both the polymer charge density and the nature of the surface. The interaction between the polyelectrolyte and gold proved to be significantly stronger than that with silica, rendering the polymer layer more resistant to damage under shear and, consequently, a significantly different friction−load relationship. The dynamics of the interactions were also investigated and were highly dependent on the polyelectrolyte−surface interaction. As an aside, a novel observation of interference effects between cantilever and substrate is also made.

Introduction

Polymers have long been used as additives to systems to act as stability, adhesion, and friction modifiers, and much work has been invested in understanding structure−property relationships. Many useful reviews have been written on the subject of polymers at interfaces, which cover work investigated over many years and by a multitude of authors.[1−3]

One important application of polymers is as steric stabilizers, which is achieved by adsorbing (or alternatively grafting) polymers at an interface in such a way that they are able to prevent two surfaces from coming close enough for attractive van der Waals (vdW) forces to cause coagulation. This requires that the polymer segment−segment interactions are repulsive and that the dielectric properties of the layers including solvent reflect those of the bulk rather than the substrate. This process is in general well understood; however, the effect of steric layers on lateral forces, particularly in polyelectrolyte systems, is much less studied. Recent articles on the subject[4−7] do however show that progress is being made in this important area including such responses as shear-melting[8] and energy losses due to deformation and alignment of viscoelastic films.[9]

Over the past few years our group has devoted a great deal of effort to the study of the relationship between polyelectrolyte composition/substrate chemistry and normal surface forces, and the consequent information on adsorption conformation that can be inferred.[10−13] More recently these studies have been complemented by dissipative quartz crystal microbalance (QCM-D) studies.[14,15] Together with the previous paper in this series, this work constitutes our first foray into the relationship between the structure of the adsorbed layer and the consequent friction force behavior.

It is the conformation of the adsorbed polymer that determines the nature and range of the surface forces (both lateral and normal), and this in turn is determined by the properties of the polymer and the substrate. Enough is now known about how the adsorbed conformation can be controlled through polyelectrolyte charge, solvent composition, temperature, etc. that this can be quite efficiently tuned to allow lateral force conformation studies. The importance of (often ignored) dynamic effects in these systems, due to the viscoelastic nature of polymers, is another parameter that needs to be considered.

* To whom the correspondence should be addressed. E-mail: mark.rutland@surfchem.kth.se.

(1) Patel Sanjay, S.; Tirrell, M. *Annu. Rev. Phys. Chem.* **1989**, *40*, 597−635.
(2) Luckham, P. F.; Klein, J. *Adv. Colloid Interface Sci.* **1997**, *73*, 1−46.
(3) Jones, R. A. L.; Richards, R. W. *Polymers at surfaces and interfaces*, 1st ed.; Cambridge University Press: Cambridge, 1999.
(4) Raviv, U.; Tadmor, R.; Klein, J. *J. Phys. Chem. B* **2001**, *105*, 8125−8134.
(5) Luengo, G.; Schmitt, F.-J.; Hill, R.; Israelachvili, J. *Macromolecules* **1997**, *30*, 2482−2494.
(6) Baker, S. M.; Smith, G. S.; Anastassopoulos, D. L.; Toprakcioglu, C.; Vradis, A. A.; Bucknall, D. G. *Macromolecules* **2000**, *33*, 1120−1122.
(7) Feldman, K.; Fritz, M.; Hähner, G.; Marti, A.; Spencer, N. D. *Tribol. Int.* **1998**, *31*, 99−105.
(8) Gee, M. L.; McGuiggan, P. M.; Israelachvili, J.; Homola, A. M. *J Chem. Phys.* **1990**, *93*, 1895.
(9) Luengo, G.; Israelachvili, J.; Granick, S. *Wear* **1996**, *200*, 328.
(10) Dahlgren, M. A. G.; Waltermo, Å; Blomberg, E.; Claesson, P. M.; Sjöström, L.; Åkesson, T.; Jönsson, B. *J. Phys. Chem.* **1993**, *97*, 11769−11775.
(11) Dahlgren, M. A. G.; Hollenberg, H. C. M.; Claesson, P. M. *Langmuir* **1995**, *11*, 4480.
(12) Poptoshev, E.; Claesson, P. M. *Langmuir* **2002**, *18*, 1184−1189.
(13) Abraham, T.; Kumpulainen, A.; Xu, Z.; Rutland, M.; Claesson, P. M.; Masliyah, J. *Langmuir* **2001**, *17*, 8321−8327.
(14) Plunkett, M. A.; Claesson, P. M.; Rutland, M. W. *Langmuir* **2002**, *18*, 1274.
(15) Plunkett, M. A.; Ernstsson, M.; Claesson, P. M.; Rutland, M. W. Submitted for publication.

10.1021/la026571h CCC: $25.00
Published on Web 04/18/2003

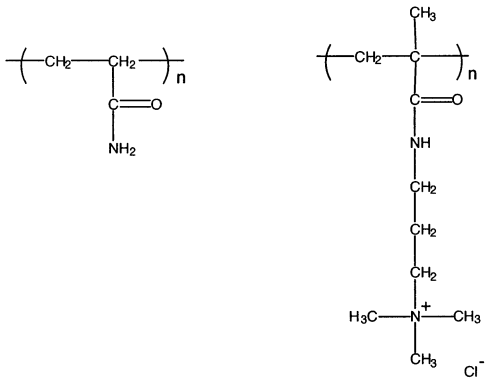

Figure 1. Schematic representation of the monomers AM (left) and MAPTAC (right).

Materials and Methods

Materials. As in paper 1,[16] analytical grade KBr and Milli-Q water were used in all solutions. Polished silicon wafers, thermally oxidized to produce a SiO_2 layer of 170 nm, were kindly provided by Dr. Stefan Klintström (University of Linköping, Sweden). The silica substrates were cut to into 1 cm squares, cleaned by thorough rinsing in water then ethanol, and then plasma treated (PDG-32G plasma cleaner, Harrick Scientific Corp., USA) on medium setting for 1 min. A second lower surface was made from the above silica wafers, coated in a 100 nm thick layer of gold via an evaporation process under high vacuum.

Polymer Solutions. In all experiments, a background electrolyte of 10^{-4} M KBr in Milli-Q water was used. Two polymers were used in the study. The first was a 900 000 g/mol molecular mass, random copolymer consisting of 99% acrylamide (AM) and 1% [3-(2-methylpropionamide)propyl]trimethylammonium chloride (MAPTAC). The AM is an uncharged monomer while the MAPTAC is positively charged leading to a charge density of 1% of monomers. The second polymer was a 248 000 g/mol molecular weight homopolymer of the charged MAPTAC monomer, which by convention is referred to as AM-MAPTAC-100% (even though the polymer contains no acrylamide). Schematics of both monomers are shown in Figure 1.

Methods. *Atomic Force Microscope.* The atomic force microscope used in these experiments was a Nanoscope IIIa Multimode atomic force microscope (Digital Instruments, Santa Barbara, USA) equipped with a fluid cell. Solutions were sucked into the cell through the inlet port (via Teflon tubing) by using a syringe attached at the *outlet* port in order to reduce contamination and air bubbles.

Colloidal Probe. Attachment of spherical micrometer-sized particles to the atomic force microscope cantilevers is now common practice.[17,18] In this work, silica beads ($R \approx 10$ μm, determined by optical microscope, Duke Scientific Corp., USA) were attached to tipless rectangular cantilevers (CSC12, MikroMasch, Estonia) using a very small amount of quick-setting, two-part epoxy resin (Araldite). The glue and spheres were applied to the cantilever by etched tungsten wires attached to a micromanipulator arm, under microscopic control (Nikon, Japan). The cantilevers were left for at least 12 h to allow the glue to fully cure. Immediately prior to measurement, the colloid probe was cleaned by rinsing in Milli-Q water and then ethanol, then blown dry under nitrogen, and finally plasma treated (PDG-32G plasma cleaner Harrick Scientific Corp., USA) on medium setting for 1 min.

Spring Constant Calculations. The cantilevers' normal spring constants were determined from the change in resonant frequency upon attachment of a series of tungsten spheres (minimum three) to the end of the cantilever.[18] The normal spring constants were determined to be 4.2 ± 0.6 N/m. A linear correlation was observed between the resonant frequency of the loaded and unloaded cantilever.

Quantitative measurements of the friction force were possible once the torsional spring constant of the AFM cantilever is known. The cantilever torsional spring constant was determined according to the calibration procedure proposed by Rutland,[19] which was shown to give identical results to the related method proposed by Feiler et al.[20] Briefly, a second cantilever with integrated tip glued on the lower surface acts as a pivot which twists the active cantilever as it is brought into contact with the pivot. The procedure was simplified by pressing the cantilever at three contact points only, one in the center line of the cantilever (where the probe was to be mounted) and one at either side as close as possible to the edge. Since the width of the cantilever could be determined accurately using optical microscopy, this avoided using the piezo movement to measure the distance. This resulted in an average value of $(3.2 \pm 0.1) \times 10^{-8}$ N m/rad for 10 cantilevers. The torsional spring constant varied between (2.7 and 4.1) $\times$ 10^{-8} N m/rad, and there was a linear correlation between the normal and torsional spring constant.

A calibration constant of the photodiode for lateral force measurement was obtained using the method of Meurk et al.[21] in which the lateral voltage signal was recorded as the laser beam moved laterally across the photodiode using the stepper motor to tilt a mirrored substrate.

Friction Measurements. The friction force was calculated from so-called friction force loops by taking the average friction force between the forward and reverse scan directions as the substrate was moved under the colloid probe. In all measurements a scan size of 5 μm was used. The friction force was measured as a function of increasing then decreasing load. Also for some measurements, the applied load was kept constant as the scan rate was varied.

Results

Bare Substrates. Surface force and friction interactions between the two silica surfaces have been presented in paper 1[16] and will not be discussed further here other than in comparison to the new systems investigated in this work. The interaction between a silica sphere (the same type as in the silica/silica case) and a gold-coated (100 nm) silica wafer, however, was found to be completely different. In this case the normal surface forces (depicted in Figure 2) did not show a double layer repulsion but instead an attraction out to 50 nm separation was observed which is too long ranged to be explained only by a van der Waals (vdW) interaction. An ordinary vdW interaction, calculated using Lifshitz theory with a Hamaker constant of 1×10^{-19} J is shown in Figure 2 for comparison, as is a DLVO interaction between a surface of -85 mV and a second of $+15$ mV for both constant charge (upper) and constant potential (including vdW interaction). The decay length has been set as $2\kappa^{-1}$ to mimic a charge image type interaction and has consequently also been calculated for two spheres. While no claim is made that this is an accurate theoretical description of the system, it indicates clearly that the forces are broadly consistent with image charging, whereas a vdW attraction is clearly an inadequate description.

The friction measurements for the bare gold/silica system are significantly lower than those obtained for the interaction between two silica surfaces ($\mu = 0.23$ and $\mu = 0.59$ at 1 Hz, respectively); both cases showed a linear friction response with load.

Varying Substrate, Au−Silica 1%AM-MAPTAC. *Forces.* In paper 1, we investigated the interaction between

(16) Feiler, A.; Plunkett, M. A.; Rutland, M. W. *Langmuir* **2003**, *19*, 4173−4179.

(17) Ducker, W. A.; Senden, T. J.; Pashely, R. M. *Nature* **1991**, *353*, 239.

(18) Ducker, W. A.; Senden, T. J.; Pashely, R. M. *Langmuir* **1992**, *8*, 1831.

(19) Bogdanovic, G.; Meurk, A.; Rutland, M. W. *Colloids Surf., B* **2000**, *19*, 397−405.

(20) Feiler, A.; Attard, P.; Larson, I. *Rev. Sci. Instrum.* **2000**, *71*, 2746−2750.

(21) Meurk, A.; Larson, I.; Bergström, L. In *Fundamentals of nanoindentation and nanotribology*; Moody, N. R., Gerberich, W. W., Baker, S. P., Burnham, S. P., Eds.; Materials Research Society: Pittsburgh, PA, 1998; Vol. 522, pp 427−432.

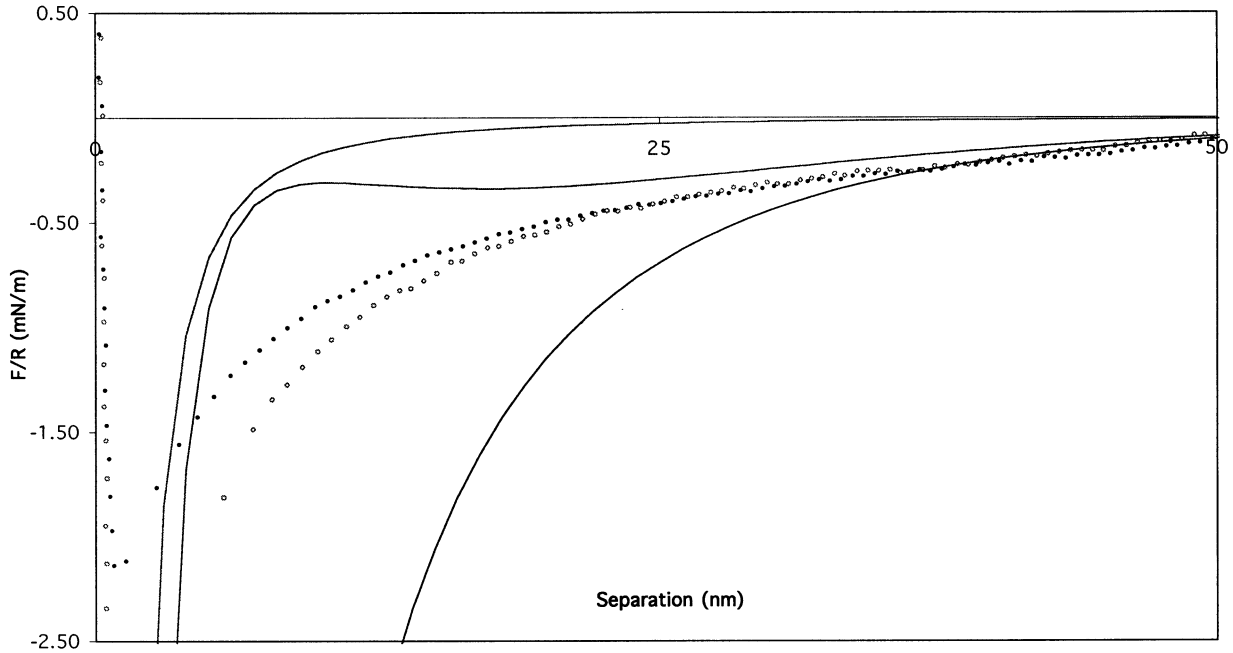

Figure 2. Surface forces as a function of separation for the interaction between a 100 nm gold coated lower substrate and a 20 μm silica sphere. The solid symbols are for approach data and the open symbols for the retraction. The additional curves are theoretically calculated. The top is for the van der Waals interaction with a Hamaker constant of 1×10^{-19} J. The other two are for DLVO interaction at constant charge and potential, respectively, which have been calculated as a first approximation to a charge image interaction.

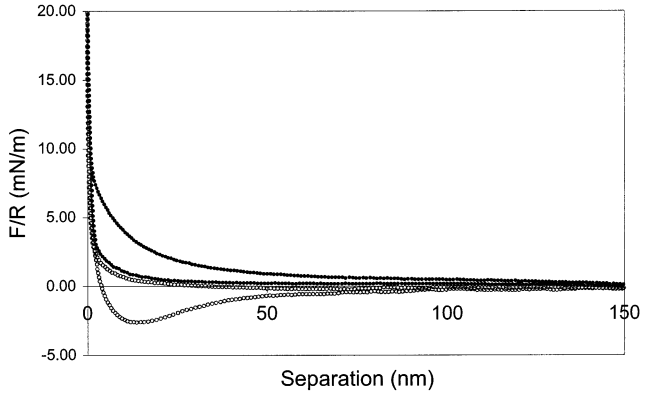

Figure 3. Force as a function of separation for AM-MAPTAC-1% adsorbed onto a gold lower surface and a silica sphere. Solid symbols are for forces on approach, and open symbols are for retraction. The middle data curves are for 1 Hz interactions while the outer data are at 14 Hz.

two silica surfaces coated with AM-MAPTAC-1%. In this case we have performed the same measurements, only substituting a gold-coated silica wafer for the lower silica surface. The normal forces for this system are shown in Figure 3, for rates of both 1 and 14 Hz (1 μm piezo expansion). There is a large reduction in the range of the steric force compared to the symmetrical silica case indicating that on the gold surface the conformation of the polyelectrolytes is more compact. Similarly to the previous symmetrical silica case, the force curves are hysteretic between approach and retraction. In paper 1[16] this effect was attributed to a hydrodynamic drainage effect, greatly enhanced by the effective viscosity increase caused by solvent flow within the polymer network. The only difference is that no hysteresis was observed at 1 Hz in the previous work. In this case the small hysteresis at slow rates appears to be consistent with either slight bridging or intersurface entanglement since it is adhesive at long range and small steps occur which are indicative of individual chain pull-off.

Friction. Although the normal force curves are qualitatively similar irrespective of the lower substrate nature, the friction behavior is significantly different. At low shear rates the frictional behavior is to all intents and purposes linear with increasing load and returns a high friction coefficient of $\mu = 0.72$ (see Figure 4) This compares to a value of $\mu = 0.59$ between silica surfaces and $\mu = 0.23$ between gold and silica (which is also included in the figure). As the shear rate is increased, the frictional behavior is approximately unchanged below a load of 300 nN but at that point deviates to an apparently nonlinear regime with considerably shallower gradient, indicating lower frictional characteristics. At 10 Hz this lower friction regime runs approximately parallel to the case of 5 Hz (indicating a similar effective friction coefficient) but at even lower absolute values of friction indicating that the load threshold is even lower than that at higher shear. Finally these effects are demonstrably not due to permanent damage, since when the rate is returned to 1 Hz the behavior is almost identical to that observed prior to the rate experiments.

Adsorbed Layer Structure Effects (AM-MAPTAC-100%). *Normal Forces.* The normal surface forces for the case of adsorbed AM-MAPTAC-100% for either silica/silica or gold/silica are shown in Figure 5. In both cases the polymer is seen to adsorb in a flat, almost incompressible layer (in contrast to the steric layer seen for the 1% charged polyelectrolyte). In the gold surface case, there is virtually no force prior to the constant compliance (the region defined as contact of the surfaces for analysis[17]); however, for the silica/silica case, there is a significant double layer repulsion (see inset with fit to a surface potential of 90 mV) and also a small hysteresis between the approach and retraction which suggests that the polyelectrolyte layer is affected by the compressional forces applied during the measurement. In addition, for the silica case at very slow rates (0.01 Hz), there is a small increase in adhesion

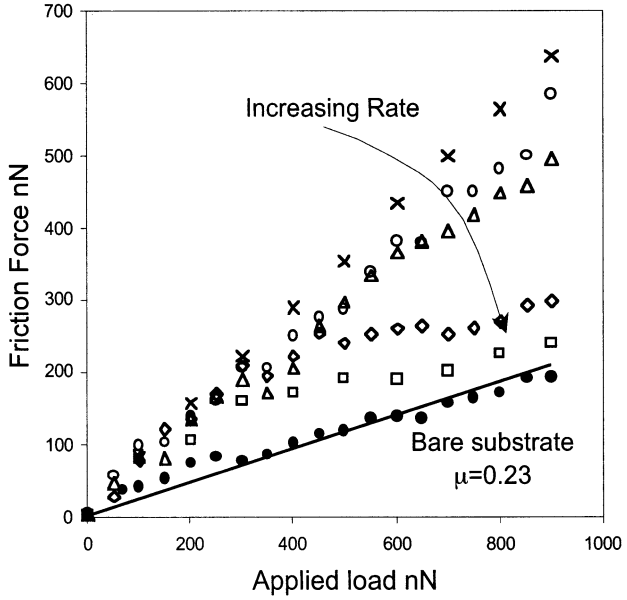

Figure 4. Friction as a function of load for AM-MAPTAC-1% adsorbed onto gold/silica substrates. The lower curve (solid circles) is the bare substrates and is fitted to a linear trendline to give a friction coefficient of 0.23. The other curves are for various friction rates after the introduction of AM-MAPTAC-1% to the system (represented with open symbols). The rates in the order conducted are as follows: 1 Hz (circles) 2 Hz (triangles), 5 Hz (diamonds), 10 Hz (squares) and 1 Hz repeat (cross). The arrow represents the effect of rate.

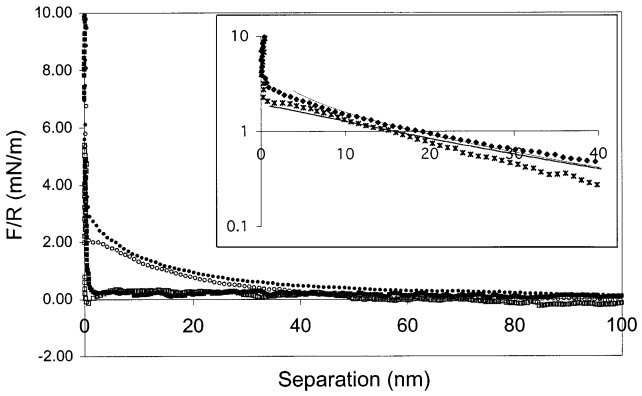

Figure 5. Force vs separation curves for adsorbed layers of AM-MAPTAC-100%. Solid symbols are for approach while open symbols are for the retraction. The upper curves (circles) are for silica substrates and the lower curves (squares) are for when the lower surface is replaced by gold. The inset shows the data for the silica system from the main figure on a semilog plot with a fit to DLVO theory at constant charge and constant potential (surface potentials of 90 mV).

(less than 1 mN/m), which is likely due to the onset of bridging forces.

After the measurement of the friction curves, the normal forces were re-examined as a way of detecting whether the shearing motion had caused any permanent changes to the adsorbed layers. In the case with gold substrates there were no significant changes in the measured forces. However, for the case with silica substrates (Figure 6), a significant pull-off force was seen. Interestingly, this adhesion displayed dynamic behavior and increased with decreasing approach rate. Note that a decrease in rate also causes an increased contact time. The point at highest rate appears to be at a slightly larger value than that at 1 Hz, but this small upturn is due to a dynamic artifact caused by an increased hydrodynamic attraction between

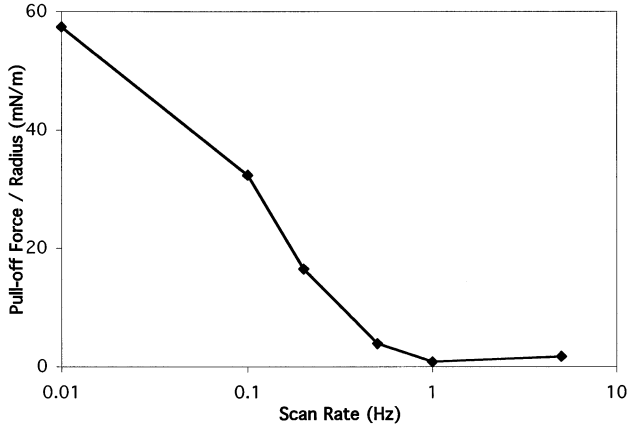

Figure 6. Pull-off vs scan rate for AM-MAPTAC-100% adsorbed onto silica substrates after friction measurements. Before the shear motion of the friction measurements, there is no significant adhesion; the curve shifts to the right as the amount of shear to which the surfaces are exposed increases.

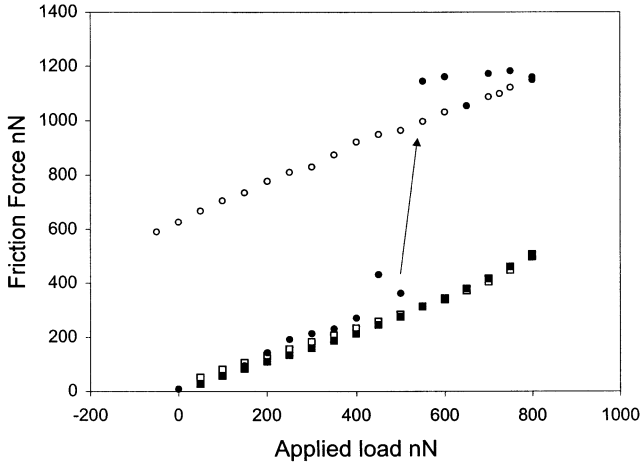

Figure 7. Friction−load relation for bare silica substrates (squares) and with the addition of AM-MAPTAC-100% (circles). Solid symbols are for loading and open symbols for unloading. The arrow indicates the jump in friction due to the creation of bare substrate.

the surfaces at high rates.[16,22] Finally, the rate at which the adhesion increases after friction depends on the history of the friction measurements. If the surfaces are sheared for a longer time, then the curve shifts to the right, indicating that as friction continues, the change to the layers becomes more pronounced.

Friction. AM-MAPTAC-100% Adsorbed onto Silica Surfaces. Figure 7 shows that the friction at 1 Hz (low shear rate) is initially linear with load and displays a very similar friction coefficient to the case without polymer. At around 400−500 nN there is a sudden very large increase in the friction. Significantly this is at the same load that caused a similar increase in friction for AM-MAPTAC-1% on silica; see paper 1.[16] However, unlike the case of the low charge density polymer, the system does not recover between runs. Furthermore, in the case of the high charge polymer, the friction force persists even at negative loads indicating an adhesion between the surfaces (as confirmed in the force curves Figure 6).

In Figure 8 the same polymer system from Figure 7 is subjected to continued shear (i.e., the data in Figure 8 are recorded directly after that found in Figure 7). In this case the hysteresis between unloading and loading curves

(22) Chan, D. Y. C.; Horn, R. G. *J. Chem. Phys.* **1985**, *83*, 5311−5324.

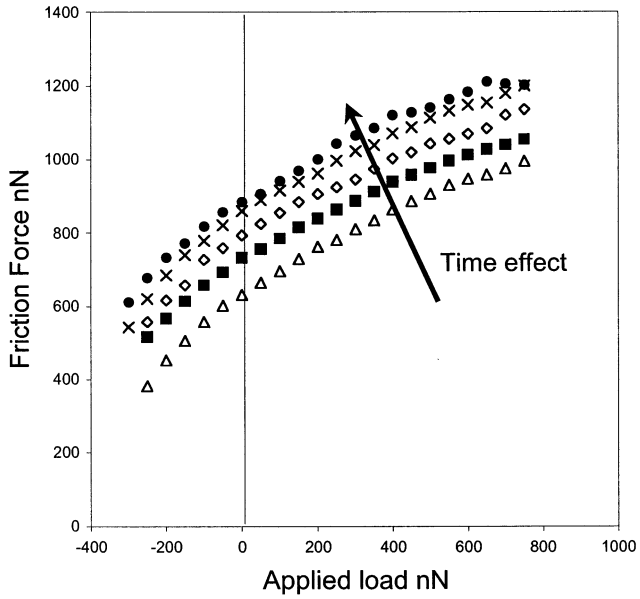

Figure 8. Friction as a function of load (loading and unloading) for AM-MAPTAC-100% adsorbed onto silica surfaces. The rates in the order conducted are, 2 Hz (open triangles) 3 Hz (solid squares), 5 Hz (open diamonds), 10 Hz (crosses), and 1 Hz repeat (circles). The arrow shows the direction of time in the measurements that leads to a constant increase in the friction. It is also noted that on unloading that the friction continues at negative loads.

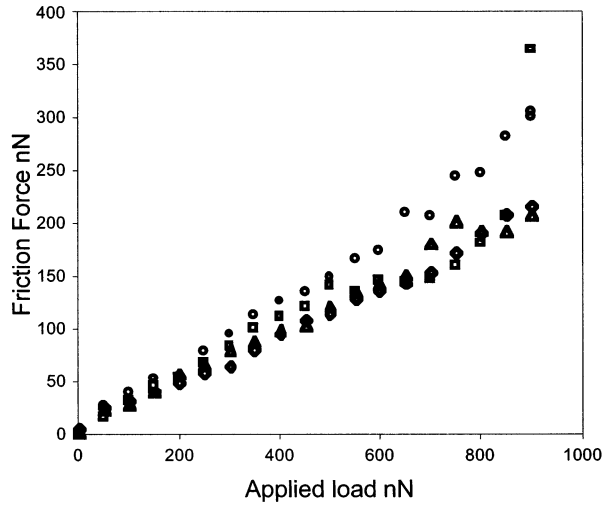

Figure 9. Friction-load relation for AM-MAPTAC-100% with a gold lower surface. The rates in the order conducted are 1 Hz (circles) 2 Hz (triangles), 5 Hz (diamonds), and 10 Hz (squares).

disappears, yet there is a temporal effect which leads to an increase in the friction over time. The friction also persists to increasingly negative loads.

AM-MAPTAC-100% with Gold-Coated Lower Substrate. In this case the friction was low over the entire course of investigation and no significant effects were found due to shear rate, except possibly slightly enhanced friction at lower rates (see Figure 9). The friction−load relation was found to be roughly linear over the entire range, with a friction coefficient of between 0.24 and 0.35.

Discussion

Normal Surface Forces. The long-range attraction seen in the gold/silica normal surface forces can be explained by two possibilities, both of which involve electrostatics. First it could be a double layer attraction. However, this would require that the gold has a positive charge since silica is known to be negatively charged in aqueous solution at this pH. Since gold is usually also thought to be intrinsically negatively charged,[23] this renders the first suggestion unlikely. The second possibility is that charge image effects, which have been invoked in the past to explain the high affinity of polyelectrolytes to the gold surface, dominate the interaction between the two surfaces.[14] As illustrated in Figure 2, the data were fitted with a DLVO-type interaction which was modified by assuming charge image interaction. Further analysis was not conducted as this lies outside the scope of the current work. Note that the use of the gold substrate engenders significant optical noise and this would also render more advanced theoretical treatments difficult.

The reason for the high optical noise levels in the experiments was 2-fold. As is seen in Figure 10, the normal optical noise of wavelength roughly 252 nm in water (lower curve) was decreased by a factor of 2 when the laser was focused onto the cantilever (upper curve), most likely due to an interference between the substrate and the back of the cantilever. The intermediate case shows a signal with both wavelengths. The schematics to the right in this figure, attempt to illustrate the likely mechanism. The bottom figure is for the commonly observed optical noise. In this case the laser is reflected from both the cantilever and the lower substrate. As the lower surface approaches the cantilever, the relative phase between the two beams changes and hence optical interference is measured, with a wavelength half that of the laser in water (since it travels the distance between the cantilever and substrate twice). Focusing the laser beam onto the middle of the cantilever and hence minimizing the intensity of the substrate reflection ordinarily remove this effect. When this is done in the present case, however, the wavelength of the optical interference is doubled not removed. We believe this is due to the laser in part passing through the cantilever, reflecting off the lower substrate, then reflecting off the cantilever again such that the path length of the secondary beam is now four times the separation between the lower substrate and the reflective coating on the cantilever, as illustrated in the upper schematic in Figure 11.

By comparing the normal surface force results for the AM-MAPTAC-1% adsorbed onto a silica wafer to that on a 100 nm gold layer (both against the same polymer layer adsorbed onto a silica sphere), it is clear that the substrate has a significant effect on the conformation of the adsorbed polymer layer. The considerably shorter ranged forces in the case of gold are indicative of a compacted layer. The electrical properties of the gold surface are such that image charges can form on the approach of a charged species. Thus the gold surface is not limited to a fixed number and distribution of charged binding sites (as is the case for silica), and a larger fraction of an adsorbing polyelectrolyte's charged groups can interact electrostatically with the surface.

As expected, changing to the highly charged AM-MAPTAC-100% led to significant differences in the forces measured on both substrates. For both substrates the polymer layer was shown to undergo very little compression, which is in agreement with previous surface force apparatus (SFA)[10,24−26] and measurement and analysis of

(23) Ederth, T. In *Chemistry*; Kungl Tekniska Högskolen: Stockholm, 1999.

(24) Rojas, O. J.; Neuman, R. D.; Claesson, P. M. *J. Colloid Interface Sci.* **2001**, *237*, 104−111.

(25) Kjellin, M. U. R.; Claesson, P. M.; Audebert, R. *J. Colloid Interface Sci.* **1997**, *190*, 476−484.

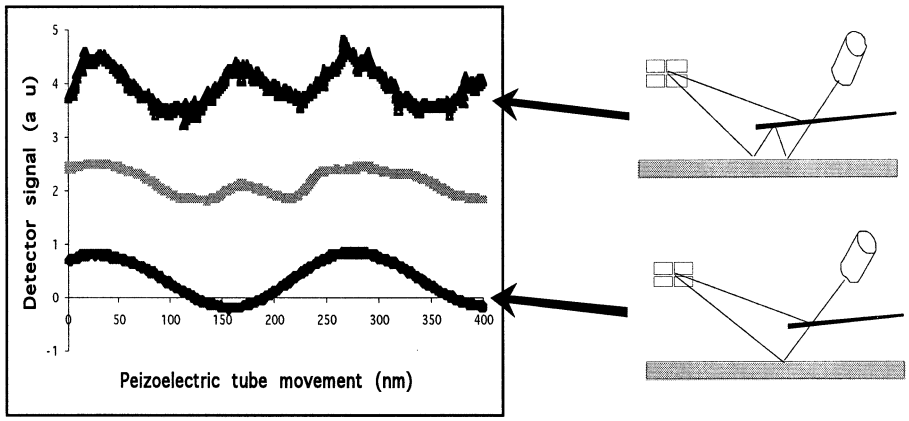

Figure 10. Comparison of optical interference wavelengths. The *y* values have been adjusted and offset for clarity. From bottom to top, the signals were obtained for the laser spot aligned (i) at the end of the cantilever with half the spot falling on the lower surface, (ii) exactly at the end of the cantilever, and (iii) position back from the end by around 10 μm (equivalent to the spot size). Note the change in the wavelength by a factor of 2 going from a single reflection to a double reflection. The intermediate case ii is due to a composite of both interference patterns. The schematic indicates a proposed mechanism as discussed in the text.

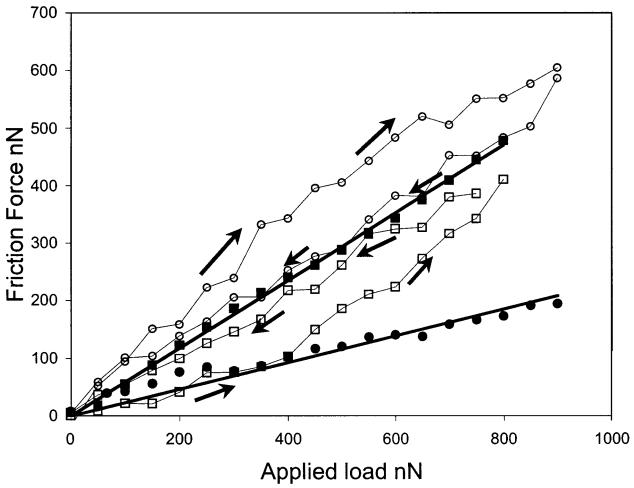

Figure 11. Friction as a function of load at 1 Hz. The squares represent the silica−silica system and the circles represent the gold−silica system. Solid symbols are for the bare substrates, and open symbols are for with AM-MAPTAC-1%. The linear trend lines for the bare substrates are added to determine friction coefficients of 0.59 and 0.23, respectively. The arrows indicate the load direction (loading or unloading) for the polymer cases.

surface interaction forces (MASIF)[12] studies and has been inferred by QCM[14,15] results. The main difference between the normal forces measured on the two different substrates was that in the case of the gold surface, the double layer repulsion seen for the silica case was absent. This suggests that the AM-MAPTAC-100% polymer coated gold surface is neutral in charge. As discussed in some of the above references, adsorption of the highly charged polyelectrolyte leads to a thin, rigid layer due to the strong attractive interaction between the multicharged cation and the negative surface and concurrently strong intermolecular repulsion which makes overcompensation of the underlying surface difficult once initial adsorption occurs.

One of the significant differences between the normal forces measured on the two substrates was that for the silica/silica system, friction measurements were able to affect subsequent force measurements. In contrast, for the gold substrate, the normal forces did not alter markedly after shear. This agrees well with QCM results[14] which show that the polyelectrolytes have a higher affinity for the gold surface, compared to mica or silica. Again, the presence of image charging on gold means that the adsorbed molecules have a larger number adhesive contacts.

This effect of the friction on the force curves on silica was shown to be significant. In the case of the AM-MAPTAC-100%, it leads to a large increase in adhesion which increases with a decrease in measurement speed. Since we are applying a simple triangle wave in all experiments, a decreased rate naturally leads to an increased contact time. Since the most likely explanation for the adhesion is intersurface bridging by the polyelectrolyte, this means that the polymers have more time to locate vacant adsorption sites on opposing surfaces. The corollary of this argument is that the shearing process must have created vacant sites on at least one of the surfaces through either removal of material or significant orientational changes and probably also that the layers are rather thin. The longer time exposed to shear, the greater the adhesion measured and thus the more silica surface sites that must have been exposed. Thus in contrast to an initial and permanent shear-induced conformational change as observed for the 1% case,[16] we see evidence of a gradual wearing process. By the same token this wearing process is quite slow—within a friction rate experiment such as that seen in Figure 8, the friction behavior returns to the same value after a rate "loop".

The fact that the adhesion does not significantly increase for the gold/silica system is possibly unexpected since in that case there is still one silica surface. We suggest that there are two possible explanations. First is that the silica spheres are significantly different in character to the silica wafers, resulting in a difference in the affinity of the polyelectrolyte on the two substrates. Second and perhaps more importantly, we note that the effect of the friction measurement on the two substrates is different. The upper sphere drags across the lower surface, in this case traveling over a 5 μm trace. The upper surface itself, however, only really has two contact areas during sliding friction, which are around 50−100 nm from the central position (determined by the tilt associated with the friction and thus dependent on both the amount of friction and the torsional spring constant). This places the contact positions during sliding well away from the contact position during normal force measurements. This distance is also possibly larger than the length of any possible loops that may lead to

(26) Fielden, M. L.; Claesson, P. M.; Schillen, K. *Langmuir* **1998**, *14*, 5366−5375.

bridging. Since the polyelectrolyte has a higher affinity for the gold substrate, it is also less likely for polyelectrolyte chains to leave the gold substrate to adsorb onto the upper silica sphere, bare patches or not.

Friction. The friction force between a gold surface and a silica surface was significantly lower than that between two silica surfaces. This may be related to the smoothness of the surfaces but is also likely to be dependent on the way that the surfaces are hydrated. Silica has exposed silanol groups whereas the gold surface is unlikely to have protruding hydrated groups. Another possibility, which has been discussed for the case of dry sliding,[27] is that the formation of hydrogen bonds may lead to enhanced frictional coefficients—this will not occur with a gold surface. However given that the silanol groups are hydrated, it seems unlikely that the capacity for inter-surface hydrogen bonding in water is very large unless it occurs between hydration ion shells, but this would show up in force measurements. It is also possible that the effective lattice spacing at the atomic level is different between the two, and thus energy dissipation is lower in terms of a "cobblestone model" type friction mechanism.[28]

For the 1% charged polyelectrolyte, a significantly different friction was seen with a gold lower surface. To compare the friction for bare substrates against the systems with AM-MAPTAC-1%, we have plotted the results for the 1 Hz rates in Figure 11. As discussed previously[16] for low loads, under 400 nN, the friction for the AM-MAPTAC-1% polymer on silica is substantially lower than after the threshold load. In this case the polymer on silica is similar to the gold−silica curve. It is of interest to note that the cases with polymer (other than at low load on silica) lie on either side of the bare silica interaction, yet the bare gold/silica interaction has substantially lower friction. Since the layer is more stable and compressed on gold, there is no load-induced change in the friction regime (over the loads investigated) compared to that seen without the gold surface.[16] Since the electrosteric layer with associated solvent is able to maintain the integrity of its conformation, it is able to act as a lubricant (mixed lubrication regime), instead of increasing the drag on the surface and hence increasing the friction with rate due to the viscoelasticity of the layer (as in the case for 1% charged polymer on silica).[16]

Changing the affinity of the polyelectrolyte for the surface, by increasing the charge density from 1% to 100% not only changed the conformation (from extended to flat) but it also had a significant affect on the measured friction. For the case of two silica surfaces, it was seen that after a load of 400−500 nN in the friction (interestingly the same load that disrupted the 1% charged polymer conformation) there was a sudden large increase in the friction (Figure 7). After the initial cycle (in which the jump occurs, the friction was nonhysteretic (loading versus unloading) and resulted in friction at negative loads. The friction did increase between runs (over time) and had a less significant rate dependence. From the normal force curves, a bridging mechanism was seen to increase adhesion after friction; thus it is assumed that the bridging mechanism also causes the large friction increase even during sliding. The mechanism behind the bridging in friction is however different from that in normal force curves, since the time available to form bridges shown in the normal force curves is significantly higher than that in friction experiments. To this end, we propose a new model for this case. Since the upper surface is dragged along the lower surface, we suggest that it is able to drag along a series of polyelectrolyte loops, which are pulled along the lower surface in a manner similar to the ends of a mop as the mop is dragged along a floor. This allows the polyelectrolyte chains to remain in contact to the lower surface, reducing the time it takes to diffuse to the surface, which is the main time delay for adhesion in normal force curves. This MAPTAC "mop" model requires that there are bare patches on the lower surface, possibly a channel, in which the polyelectrolyte chains attached to the upper surface can adhere. The increase in friction over time is then a direct result of an increase in size of the bare patches on the lower silica surface over time. The very small rate effect in this case is most likely a viscoelastic response from the polymer. The cause of the threshold here is not well understood and may be due to removal of polyelectrolyte in some way, which would significantly increase the area of bare patches.

The friction measurements on the same polymer (AM-MAPTAC100%) with a lower surface coated in gold, in contrast show no bridging mechanism in the force curves, and hence no time related change in the frictional forces. In this case there is also no significant change in the forces as a function of scan rate. The friction coefficient for the system was between 0.24 and 0.35, which was significantly lower than the 0.59 seen between bare silica, though is similar to the value for gold/silica of 0.23. This tends to suggest that while the long-range forces change as a result of adsorption, the amount of adsorption is so small and its conformation so rigid and flat that it does not greatly modify the material properties of the surface responsible for the frictional behavior.

Conclusion/Summary

The effect of changing the lower surface from silica to gold changes not only the conformation of adsorbing polyelectrolyte but also its robustness to shear. By comparison, with two silica surfaces, the shearing process can significantly affect the polymer layer.

The affinity of the polyelectrolyte for the substrate can be reduced either by decreasing the charge density on the polyelectrolyte or by changing the substrate itself through reducing the number of possible contact points (in this case from gold, with image charge capacity, to silica). This results in the polyelectrolyte adopting a more extended layer.

When the steric layer is able to maintain its integrity, which is no doubt helped by a stronger affinity for the substrate and more compact conformation on the surface), then the layer is able to act as a lubricant in the mixed boundary/lubricant regime of the Stribeck curve. The increase in the charge density of the polyelectrolyte leads to a change in the conformation of the polymer, since it is the charged groups that have the surface affinity. For the interaction of two silica surfaces with adsorbed AM-MAPTAC-100%, the highly charged polymer adopts a relatively incompressible layer on the surfaces, which leads to a decrease in adhesion and friction. However, since the polymer is not tightly bound to the surface, friction measurements are able to alter the polyelectrolyte conformation and create bare patches on the surface. This allows for polyelectrolyte bridging between the surfaces, which leads to a strong adhesion between the surfaces. This bridging can apparently and somewhat surprisingly greatly increase the friction between the surfaces. Finally it is shown, that on gold the increased binding strength

(27) Bogdanovic, G.; Tiberg, F.; Rutland, M. W. *Langmuir* **2001**, *17*, 5911−5916.

(28) Meyer, E.; Overney, R. M.; Dransfield, K.; Gyalog, T. *Nanoscience*: *Friction and rheology on the nanometer scale*; World Scientific Publishing: Singapore, 1998.

to the surface is enough to prevent the creation of bare substrate that allows for the bridging mechanism to occur and thus keep the friction coefficient low.

There is enormously rich behavior of both friction and normal forces that can be seen by changing a small number of variables. Of particular importance is the difference in regimes that can be probed simply by changing the friction rate and the loads investigated. The mechanisms of friction and the dynamic behavior vary significantly for what might be expected to be rather similar systems.

Acknowledgment. M.P. acknowledges financial support from SSFs CIT program and A.F. acknowledges both the Swedish Research Council (VR) and Unilever Port Sunlight for their support. M.R. also acknowledges the Biofiber Material Centre, BiMaC. We are indebted to Lab. Phys-Chem Macromoleculaire, Paris for the gift of the characterized polyelectrolyte.

LA026571H